WILEY

Research Article

Assessment of Radiation Dose Associated with the Atmospheric Release of ^{41}Ar from the TRIGA Mark-II Research Reactor in Bangladesh

M. Ajijul Hoq ,[1] **M. A. Malek Soner,**[2] **S. Khanom,**[3] **M. J. Uddin,**[4] **M. Moniruzzaman,**[5] **M. S. H. Chowdhury,**[5] **A. Helal,**[5] **M. Abu Khaer** ,[6] **S. M. T. Hassan,**[6] **M. Tareque Chowdhury,**[6] **and M. Mizanur Rahman**[6]

[1]*Institute of Nuclear Medicine and Allied Sciences, Bangladesh Atomic Energy Commission, Chattogram, Bangladesh*
[2]*Center for Research Reactor, Atomic Energy Research Establishment, Bangladesh Atomic Energy Commission, Dhaka, Bangladesh*
[3]*Institute of Electronics, Atomic Energy Research Establishment, Bangladesh Atomic Energy Commission, Dhaka, Bangladesh*
[4]*National Institute of Nuclear Medicine and Allied Sciences, Bangladesh Atomic Energy Commission, Dhaka, Bangladesh*
[5]*Engineering Division, Bangladesh Atomic Energy Commission, Dhaka, Bangladesh*
[6]*Institute of Energy Science, Atomic Energy Research Establishment, Bangladesh Atomic Energy Commission, Dhaka, Bangladesh*

Correspondence should be addressed to M. Ajijul Hoq; arifstyn@yahoo.com

A major concern for nuclear research reactors under normal operating conditions is that they may release radioactive elements into the atmosphere, endangering public health and the environment. The present study concentrated on the detailed radiological dose assessment resulting from the atmospheric release of ^{41}Ar activity from the TRIGA Mark-II research reactor in Bangladesh during its normal operational condition at full power of 3 MW. The total effective dose equivalent (TEDE), ground deposition activity, organ-committed dose, and pathways dose values have been evaluated under different weather conditions using the HotSpot 3.1.2 code. The weather data have been gathered from the Bangladesh Meteorological Department (BMD), Dhaka. Two significant seasons with various weather stability effects have been considered for dose analysis. Atmospheric dispersion of ^{41}Ar was evaluated using the Gaussian plume model. From the obtained results, the maximum TEDE of 4.06×10^{-9} Sv at 0.19 km distance from the reactor site for stability class B during the summer season is found to be well below the annual effective dose limit of 1 mSv recommended by the ICRP. During the rainy season, the maximum TEDE of 1.76×10^{-9} Sv at 0.92 km distance for stability class E is also found to be negligible compared to the dose limit. From the organ-committed dose analysis, skin is investigated as the highest dose absorber compared to other organs. The pathways dose analysis concludes that the submersion and ground shine doses are observed to be maximum at 0.20 km and 1.0 km distances for the summer and rainy seasons, respectively. Based on the identified results, dose values have been found to be within the limiting values, ensuring environmental and human health safety. Such comprehensive dose analysis due to the atmospheric release of ^{41}Ar activity is very significant from the perspective of ensuring the radiological and environmental safety of research-type nuclear reactors under normal operational conditions.

1. Introduction

The Bangladesh Atomic Energy Commission (BAEC)'s TRIGA Research Reactor (BTRR) is a very significant nuclear installation in the country because it is usually used for various purposes, including basic nuclear research, materials testing, neutron radiography, and radioisotope production. The Bangladesh Atomic Energy Regulatory Authority (BAERA) licensed the BTRR, and its regulations require the facility to take all reasonable precautions to protect the

environment and the health and safety of its employees or general inhabitants, including identifying, controlling, and monitoring the release of nuclear substances into the atmosphere. Analyzing the population's total effective dose equivalent (TEDE) in the vicinity of the reactor sites under normal operating conditions is crucial for the facility's safety and environmental evaluations. Under normal reactor operational conditions, when it comes to the reactor's airborne emission of activation products, ^{41}Ar is the main product of interest which is initially generated by irradiation of dissolved air in the primary water [1]. Naturally occurring noble gas ^{40}Ar in the area surrounding the reactor vessel reacts with neutrons to produce ^{41}Ar, which is rapidly combined with air from the reactor building and ejected through the reactor stack's airflow at an effective release height of 32.36 m. During the release of ^{41}Ar activity, the actual plume height may not be the exact physical stack height as plume rise can occur due to the velocity of stack emission and the temperature discrepancy between the stack effluent and the surrounding air. After getting out from the stack, radioactive ^{41}Ar moves with local air flows offsite causing humans and the environment to be potentially exposed to gamma radiation emitted during ^{41}Ar decay. As gamma ray can pass completely through the human body, it may cause radiation effects on organs like the skin, surface bone, breast, lung, red marrow, testes, brain, thyroid, liver, and uterus. As a result, the continuous release of ^{41}Ar activity through the reactor stack during the operational stage may produce external or internal dose equivalent to the body causing radiation-induced health effects. So, it is important to investigate the radiological and environmental impact resulting from released ^{41}Ar activity during normal operational conditions which has been carried out by evaluating the comprehensive radiation doses.

In our previous studies [1, 2], assessments have been performed to estimate the ^{41}Ar activity concentration and release rate under normal reactor operation conditions with a full reactor power of 3 MW. Malek et al., 2012 [3], conducted a radiological dose distribution study due to the deposition of ^{131}I, ^{132}I, ^{133}I, ^{134}I, and ^{135}I on ground, vegetation, milk and meat considering a hypothetical accident of TRIGA Mark-II research reactor at AERE, Savar, Bangladesh. Khaer et al., 2023 [4], performed an assessment of radiological doses due to the release of radionuclides such as Xe, Kr, I, and Cs using HotSpot 3.1.2 and RASCAL 4.3 codes considering a postulated severe accident of a plane crash for the TRIGA Mark-II research reactor in Bangladesh. Mawla et al., 2024 [5], assessed radiological consequences to a hypothetical accident of the 3 MW TRIGA research reactor of Bangladesh where ORIGEN code was used to carry out the facility's radionuclide inventory, and HotSpot code was used to evaluate the TEDE. Rahman et al., 2013 [6], made an analysis of radiological doses due to the deposition of ^{137}Cs and ^{90}Sr on the ground, vegetation, milk, and meat considering a hypothetical accident at the TRIGA Mark-II research reactor in Bangladesh. Mladina et al., 2013 [7], carried out a study to develop and use a model for radioactive species transport in the primary circuit and in the reactor hall of the Romanian TRIGA facility using the CATHARE2

V25 code. Argon activity at the reactor stack was calculated for normal operation and compared to monitor readings. Fukui M., 2004 [8], performed a study for the management of the ^{41}Ar concentration in the work area in the reactor room, and as a result, a decrease in the emission from KURR was achieved.

In our previous studies [1, 2], the airborne radioisotope ^{41}Ar generation concentration, ground-level concentration, and release rate from the BTRR were evaluated during the normal reactor operation condition without any detailed dose calculation under different weather conditions considering internal and external pathways including the organ-committed dose. Therefore, the present study is going to take place in certain weather conditions with different atmospheric stability classes for a comprehensive dose study associated with the operational release of ^{41}Ar activity from the BTRR using the HotSpot 3.1.2 code. We focused our attention on the assessment of the detailed radiation dose associated with the atmospheric release of ^{41}Ar activity with potential for offsite human exposure. In our present research work, a detailed analysis of TEDE, ground deposition activity, organ-committed dose, and pathways dose has been carried out for a normal operational condition at a full reactor power of 3 MW. Yearly (2021) operational data for the BTRR have been used for the detailed dose study.

2. Materials and Methods

2.1. Atmospheric Conditions. To model the properties of the radioactive plume in the environment, weather data are needed. The required weather information includes wind direction, wind speed, atmospheric stability, and precipitation. The meteorological data for the years 1992–2021 were gathered from the Bangladesh Meteorological Department (BMD), Dhaka [9]. Meteorological data for such a long period are considered to minimize the uncertainty of the meteorological data. Wind speed and frequency are analyzed based on the raw data collected from the BMD in Dhaka. In this study, the two most significant seasons of the country have been considered for investigating the weather effects. During both the summer and rainy seasons, the dominant direction is observed to be south (S), with wind flow percentages of 92% and 65.55%, respectively. Moderate to severe rainfall is typical during the rainy season in this country. Figure 1 illustrates the percentage of wind frequencies and the average wind speed for the two different seasons. From Figure 1, the average wind speed during the summer and rainy seasons is observed to be 3.25 m/sec and 2.841 m/sec, respectively. The atmospheric stability classes range from A (very unstable) to F (moderately stable), depending on the weather condition, as given in Table 1. The stability class B has been observed during the summer season, and the stability class E has been observed during the rainy season. Due to investigating the dose variations with different weather stability effects, other atmospheric stability classes (A-F) have also been considered in this study.

TABLE 1: Atmospheric stability classes used in HotSpot 3.1.2 categories from A–F [10].

Wind speed (m/s)	Sun high in sky	Sun low in sky or cloudy	Night time
<2	*A	B	*F
2-3	A	C	*E
3-4	*B	C	D
4–6	*C	*D	D
>6	C	D	D

*Pasquill Stability Types, A: extremely unstable; B: moderately unstable; C: slightly unstable; D: neutral; E: slightly stable; F: moderately stable.
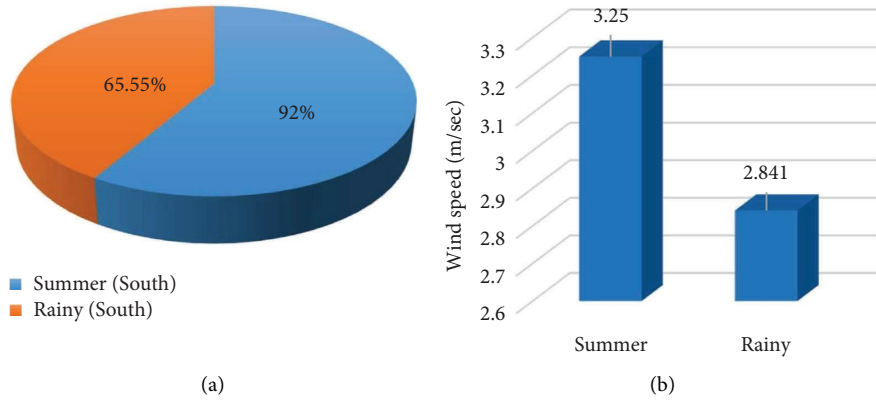

FIGURE 1: Meteorological data (a) wind frequency (%) at the dominant direction and (b) average wind speed (m/sec) during two different seasons for BTRR (1992–2021).

2.2. Site Location and Specifications of the BTRR.

The Bangladesh Atomic Energy Commission (BAEC)'s TRIGA Research Reactor (BTRR) is located at the Atomic Energy Research Establishment (AERE)'s campus which is situated at Ganakbari, Savar Upazila, Dhaka district, Bangladesh. The coordinates of the reactor are roughly 23.95° north and 90.27° east. About 10.62 meters (34.84 ft) or such is the reactor's elevation above sea level [4]. The site location of the BTRR is illustrated in Figure 2.

The BTRR is a cylindrical shaped pool-type research reactor that has been operating since September 14, 1986 [1, 11]. A few technical specifications of the BTRR have been given in Table 2.

2.3. Source Term and Reactor Operation Conditions.

Source term is crucial for determining the radioactive concentration in a nuclear research reactor. Source term refers to the amount of radioactivity released from a nuclear reactor. In our previous study [1], an assessment was performed to estimate the ^{41}Ar activity release rate from the BTRR under normal operational conditions at 3 MW reactor power. The estimated activity release rate for ^{41}Ar was 4.43×10^3 Bq/ sec [1]. In our present study, we have considered the reactor operation conditions for the year 2021, the details of which are given in Table 3. It is assumed that the reactor was in full power and that ^{41}Ar was continuously released to the atmosphere from the stack during its yearly operational period. Accounting for the reactor operating duration of about 55.47 hours, the released amount of ^{41}Ar activity is estimated by 8.84×10^8 Bq. Source term of ^{41}Ar for

the year 2021 at 3 MW$_{th}$ reactor power is contained in Table 4.

2.4. HotSpot 3.1.2 Code.

Lawrence Livermore National Laboratory (LLNL) created the HotSpot 3.1.2 code to offer a first-order approximation of the radiation effects related to the atmospheric release of radioactive materials from nuclear installations [10]. The air concentration and TEDE from radioactive emissions are computed by the HotSpot 3.1.2 code using the Gaussian plume model (GPM) [10]. The GPM has been effectively used in practice to address a wide range of dispersion issues. This is conceivable, as the general plume model is among the most extensively validated models [14]. Figure 3 illustrates the flowchart of the dose evaluation process using HotSpot code version 3.1.2. Table 5 contains a few parameters used in HotSpot 3.1.2 code for dose calculations.

It is shown in Table 5 that the effective release height of 32.36 m was used during the code analysis. During the discharging of ^{41}Ar activity into the atmosphere from the reactor building, the actual plume height may not be the exact physical stack height. Plume rise can occur as a result of the velocity of stack emission and the temperature difference between the stack effluent and surrounding air. The rise of the plume causes an increase in the release height [10]. Therefore, the term effective release height has been used during the code analysis and can be written as [15]
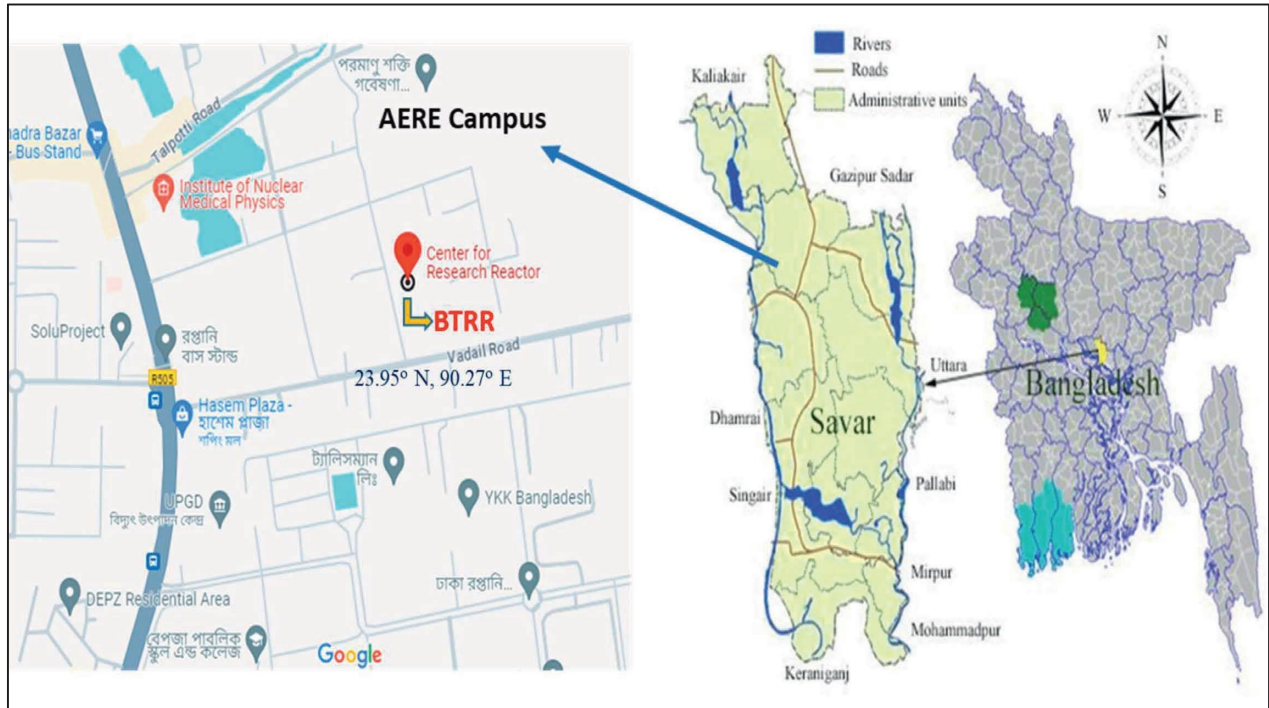
$$H = H_{\text{Actual}} + \Delta h_d, \tag{1}$$

FIGURE 2: Site location of the BTRR.

TABLE 2: Technical specifications of the BTRR [4, 12].

Parameters	Value/dimensions
Reactor type	Pool type
Coolant	Light water
Moderator	Light water
Reactor power	3 MW (th)
Uranium enrichment	19.7%
Fuel elements	$U\text{-}ZrH_{1.6}$
No. of fuel rods	100
No. of control rod	6
Control rod material	B_4C
Reactor tank	Length: 8.23 m, diameter: 1.98 m Capacity: 24,865 liters
Cladding material	SS304

TABLE 3: Operational conditions of the BTRR for dose study.

Serial no.	Type	Conditions
01	Reactor operation duration	28 days with hourly operation [13]
02	Operated power	3 MW (t)
03	Exposure duration	55.47 hours during operation [13]
04	Radionuclide	^{41}Ar ($T_{(l)} = 1.83$ hour)
05	Release fraction	100% of developed inventory in the core.

TABLE 4: Source term of ^{41}Ar for yearly (2021) reactor operation at 3 MW$_{th}$ power level.

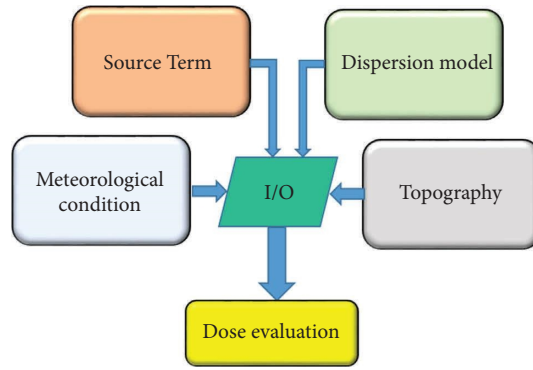| Radionuclide	Atmospheric dispersion model	Released activity (Bq)	Released rate (Bq/sec)
^{41}Ar	General plume	8.84×10^8	4.43×10^3

FIGURE 3: Flowchart of HotSpot 3.1.2 code.

TABLE 5: Parameters used in HotSpot 3.1.2 code.

	Parameters	Value
	Atmospheric dispersion model	General plume
	Source materials	^{41}Ar
	Material at risk (Bq)	8.84×10^8
	Deposition velocity (cm/s)	0.3
	Damage ratio	1
	Leak path factor	1
Dose calculations	Wind input height	10 m
	Effective release height	32.36 m
	Terrain	Standard
	Airborne fraction (ARF)	1
	Respirable fraction (RF)	1
	Sample time	10 min
	DCF library	FGR 13

where H_{Actual} is the actual stack height (m) and Δh_d is the buoyant plume rise (m).

3. Results and Discussion

The production and continuous release of ^{41}Ar activity into the environment is a regular function during normal reactor operation conditions. Based on the meteorological data, it has been determined that the frequency of the south direction is dominant and moderately unstable (Pasquill's category B) atmospheric conditions are observed frequently during the summer season. Comparable to the average human height, the receptor height was determined to be 1.5 meters. The HotSpot 3.1.2 code has been used for dose calculation. Using the GPM for atmospheric dispersion, TEDE, Ground deposition activity, organ-committed dose, and pathways dose values have been calculated using this code.

Here, Figure 4 presents the TEDE (Sv) dose values in both plume contour and plume centerline as a function of downwind distance during the summer season in stability class B for wind speed of 3.25 m/sec. From Figure 4, it is observed that the maximum TEDE (Sv) value of stability class B is 4.06×10^{-9} Sv at 0.19 km distance for wind from the South direction during the summer season. The maximum TEDE (Sv) value during the summer season is found to be lower than the annual effective dose limits set by the ICRP

[16, 17]. TEDE (Sv) values are observed to be 1×10^{-9} Sv at 0.058 km^2, 1×10^{-10} Sv at 0.75 km^2, and 1×10^{-11} Sv at 7.2 km^2 area from the TEDE (Sv) plume contour curve during the summer season. Initially, dose values are lower, then gradually increase, and reach their maximum at 0.19 km distance during the summer season. After reaching the maximum dose value, it decreases to a negligible value with the increase in distance. In our present study, we have shown that the dose distance is covered by 20 km regarding negligible dose values.

Figure 5 shows the results for calculated TEDE at various downwind distances from the BTRR site in different atmospheric stability classes (A-F) during the summer season to consider various weather stability effects. From Figure 5, a maximum TEDE of 5×10^{-9} Sv is observed for stability class A, and a minimum of 9×10^{-10} Sv is observed for stability class F during the summer season.

Here, Figure 6 presents the ground deposition activity (kBq/m^2) values in both the plume contour and plume centerline as a function of downwind distance during the summer season in stability class B for a wind speed of 3.25 m/sec. From Figure 6, it is observed that the maximum ground deposition activity (kBq/m^2) value of 1.3×10^{-01} kBq/m^2 for stability class B is found at 0.19 km distance for wind from the south during the summer season. Ground deposition values are observed to be 1×10^{-01} kBq/m^2 at 5×10^{-03} km^2, 1×10^{-02} kBq/m^2 at 0.22 km^2, and 1×10^{-03} kBq/m^2 at 2.3 km^2

Inner:
1.0E−09 Sv (0.058 km2)
Middle:
1.0E−10 Sv (0.75 km2)
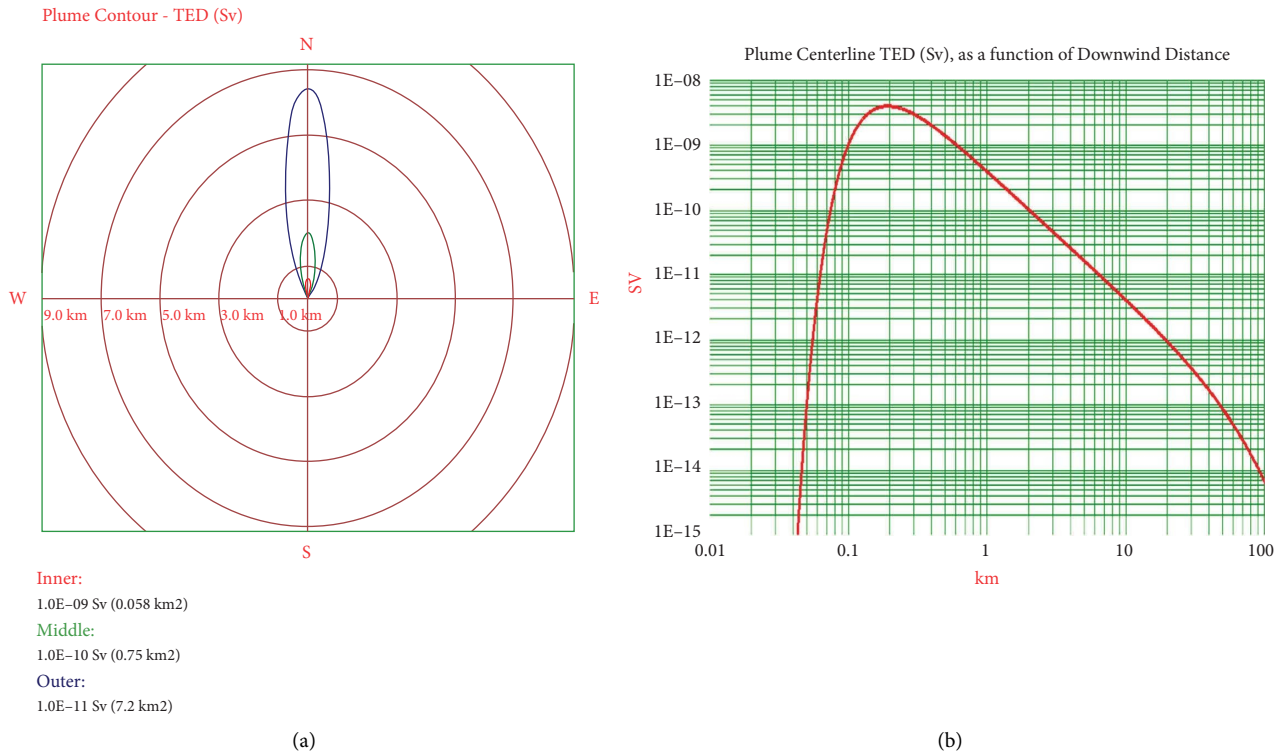Outer:
1.0E−11 Sv (7.2 km2)

(a)

(b)

FIGURE 4: TEDE (Sv) dose: (a) plume contour and (b) plume centerline as a function of downwind distance during the summer season in stability class B for the wind speed of 3.25 m/sec.
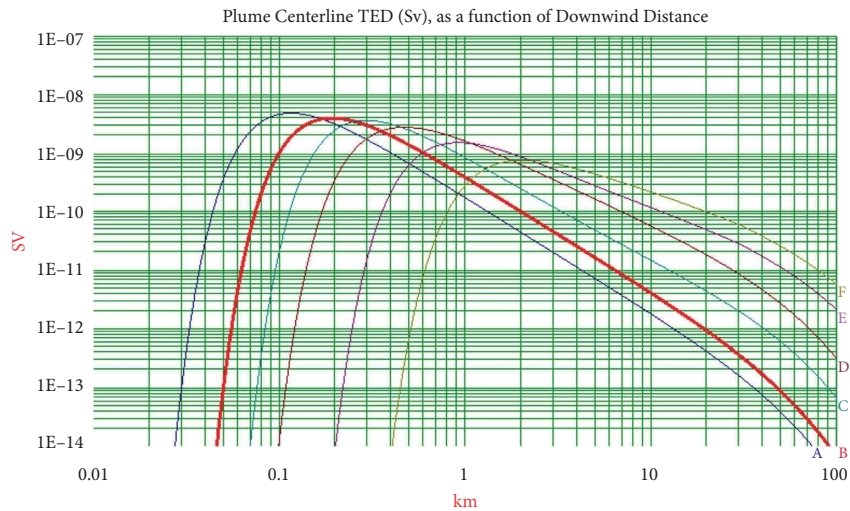

FIGURE 5: TEDE (Sv) dose as a function of downwind distance during the summer season in different atmospheric stability classes (A–F).

during the summer season. According to Figure 6, the values of ground deposition activity increase first, reach a maximum, and subsequently drop with increasing distance during the summer season.

Figure 7 shows the results for calculated ground deposition activity at various downwind distances from the BTRR site in different atmospheric stability classes (A-F) during the summer season to consider various weather stability effects. From Figure 7, a maximum ground

deposition activity of $1.7E − 01 \, \text{kBq/m}^2$ is observed for stability class A during the summer season.

HotSpot 3.1.2 permits the presentation of contours for both ground deposition (kBq/m^2) and TEDE (Sv) at the release position in Google earth. Here, Figure 8 presents the Google earth map illustration for both the TEDE (Sv) contour and the ground deposition (kBq/m^2) contour during the summer season. When the TRIGA Mark-II reactor's geographic coordinates are given into the HotSpot

Plume Contour - Ground Deposition (kBq/m2)

Inner:
1.00E−01 kBq/m2 (5E−03 km2)
Middle:
1.00E−02 kBq/m2 (0.22 km2)
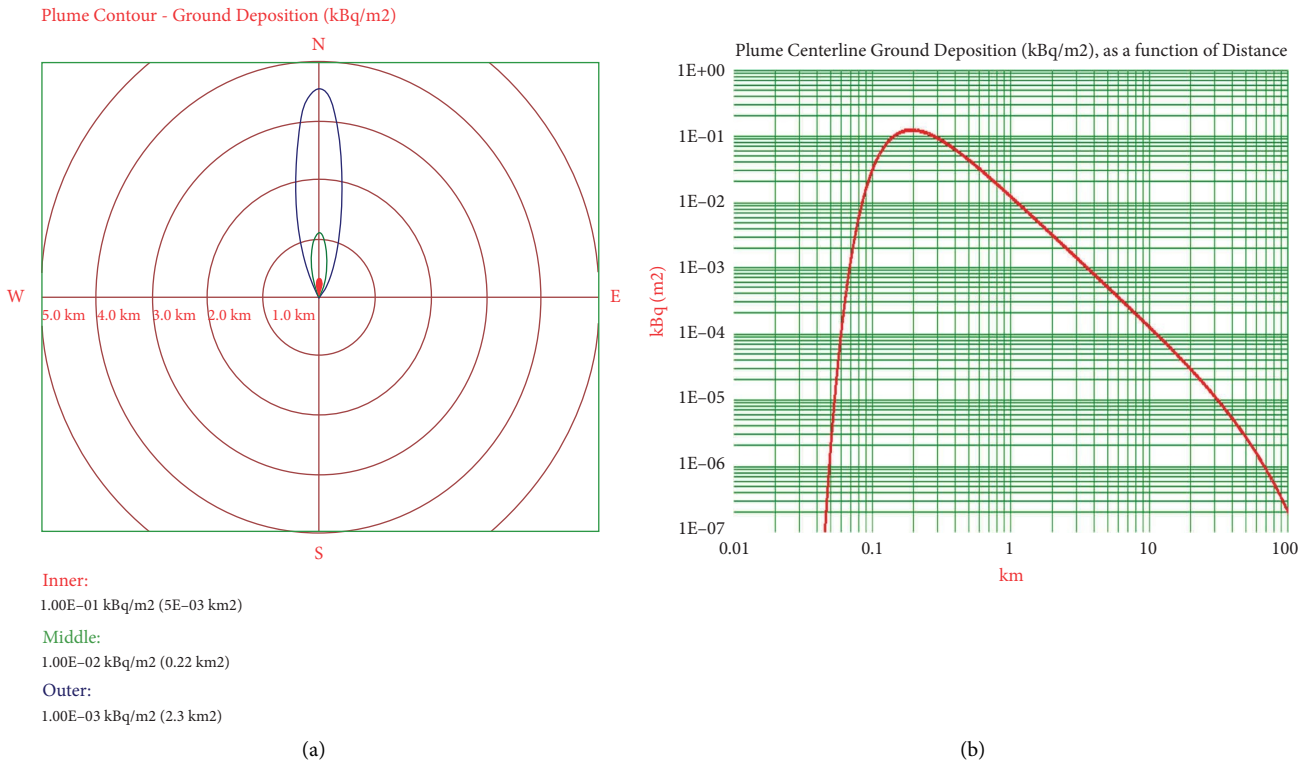Outer:
1.00E−03 kBq/m2 (2.3 km2)

(a)

(b)

FIGURE 6: Ground deposition activity: (a) plume contour and (b) plume centerline as a function of downwind distance during the summer season in stability class B for the wind speed of 3.25 m/sec.
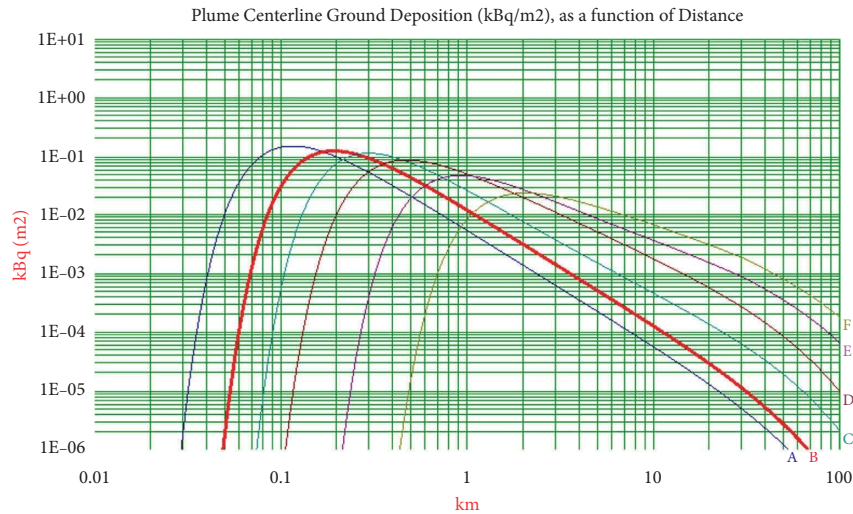
FIGURE 7: Ground deposition activity as a function of downwind distance during the summer season in different atmospheric stability classes (A–F).

3.1.2 code during the dose calculation process, the program generates Google (.kml) output, which is used to display the contour on Google map. And finally, we have plotted TEDE (Sv) plume contour and ground deposition (kBq/m^2) contour areas in Google earth pro, as shown in Figure 8, indicating the actual areas impacted by ^{41}Ar dispersion during the summer season.

The output of the HotSpot 3.1.2 code is shown in Table 6 for distances ranging from 0.03 to 20 km during the summer season. From Table 6, the maximum dose was determined at a distance of 0.20 km during the summer season. The maximum TEDE, respirable time-integrated air concentration, ground surface deposition, and ground shine dose rate are observed to be 4×10^{-9} Sv, 4.2×10^{4}

TEDE (Sv)   Ground Deposition (kBq/m^2)

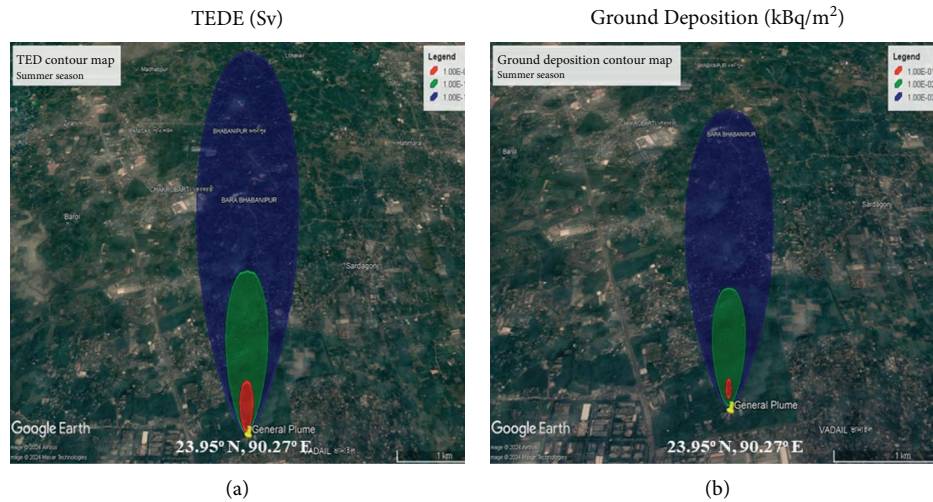(a)   (b)

FIGURE 8: Google earth map illustration of (a) TEDE (Sv) contour and (b) ground deposition (kBq/m^2) contour during the summer season.

TABLE 6: HotSpot 3.1.2 outputs for the general plume scenarios during the summer season.

Distance (km)	TEDE (Sv)	Respirable time-integrated air concentration (bq-sec)/m^3	Ground surface deposition (kBq/m^2)	Ground shine dose rate (Sv/hr)	Arrival time (hour:min)
0.030	$0.0E+00$	$2.6E-10$	$3.9E-17$	$0.0E+00$	<00:01
0.100	$1.1E-09$	$1.2E+04$	$3.3E-02$	$1.4E-10$	<00:01
0.200	$4.0E-09$	$4.2E+04$	$1.3E-01$	$5.5E-10$	<00:01
0.300	$3.0E-09$	$3.1E+04$	$9.3E-02$	$4.1E-10$	00:01
0.400	$2.0E-09$	$2.1E+04$	$6.2E-02$	$2.7E-10$	00:01
0.500	$1.4E-09$	$1.4E+04$	$4.3E-02$	$1.9E-10$	00:02
0.600	$1.0E-09$	$1.0E+04$	$3.1E-02$	$1.4E-10$	00:02
0.700	$7.6E-10$	$7.9E+03$	$2.4E-02$	$1.0E-10$	00:03
0.800	$5.9E-10$	$6.2E+03$	$1.9E-02$	$8.1E-11$	00:03
0.900	$4.8E-10$	$4.9E+03$	$1.5E-02$	$6.5E-11$	00:04
1.000	$3.9E-10$	$4.0E+03$	$1.2E-02$	$5.3E-11$	00:04
2.000	$1.0E-10$	$1.0E+03$	$3.1E-03$	$1.4E-11$	00:09
4.000	$2.6E-11$	$2.7E+02$	$8.0E-04$	$3.5E-12$	00:18
6.000	$1.2E-11$	$1.2E+02$	$3.6E-04$	$1.6E-12$	00:28
8.000	$6.5E-12$	$6.7E+01$	$2.0E-04$	$8.9E-13$	00:37
10.000	$4.1E-12$	$4.3E+01$	$1.3E-04$	$5.6E-13$	00:47
20.000	$9.3E-13$	$9.6E+00$	$2.9E-05$	$1.3E-13$	01:34

(Bq-sec)/m^3, 1.3×10^{-1} kBq/m^2, and 5.5×10^{-10} Sv, respectively, for ^{41}Ar dispersion during the summer season. The dose values are found to be very insignificant after 10 km.

Figure 9 represents the organ dose values contributed by ^{41}Ar radionuclide during the summer season. Several organs, including the skin, surface bone, breast, lung, red marrow, testes, brain, thyroid, liver, and uterus, have been taken into consideration for dose evaluation during the summer season based on the results of HotSpot 3.1.2. From Figure 9, it is observed that skin is the highest dose absorber of 1.1×10^{-8} Sv at 0.20 km distance compared to other organs during the summer season. The obtained dose value for skin during the summer season is found to be very negligible compared to the public exposure dose limit for skin of 50 mSv, as shown in Table 7.

Here, Table 7 contains the annual standard dose-limiting values for occupational and public exposure recommended by international standards.

Here, Figure 10 shows the TEDE (Sv) dose values in both plume contour and plume centerline as a function of downwind distance during the rainy season in stability class E for a wind speed of 2.841 m/sec. From Figure 10, it is observed that the maximum TEDE (Sv) value of stability class E is found to be 1.76×10^{-9} Sv at 0.92 km distance for wind from South during the rainy season. The maximum TEDE (Sv) value during the rainy season is also found to be lower than the annual effective dose limit, as shown in Table 7. TEDE (Sv) values are observed to be 1×10^{-9} Sv at 0.15 km^2, 1×10^{-10} Sv at 7.1 km^2, and 1×10^{-11} Sv at 102 km^2 area from the TEDE (Sv) plume contour curve during rainy season. Initially, dose values are lower, then
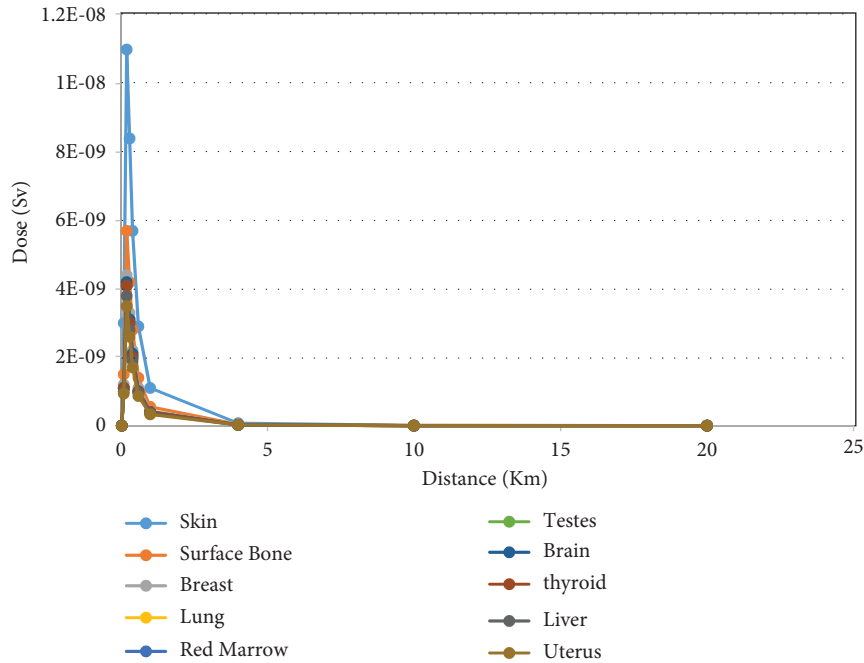
FIGURE 9: Organ-committed dose (Sv) as a function of downwind distance for Pasquill stability class B during the summer season.

TABLE 7: Dose limit for occupational and public exposure in a single year [18–20].

Radiation dose	Dose limit for adult (mSv/year)	
	Occupational exposure	Public exposure
Total effective dose equivalent (TEDE)	50	1
Whole body	50	1
Lens of the eye	50	15
Skin or extremities	500	50
Individual organ or tissue other than the lens of the eye	500	—
Pathways dose	50	1

gradually increase, and reach their maximum at 0.92 km during the rainy season. After reaching the maximum dose value, it decreased to a negligible value with the increase in distance.

The results for calculated TEDE at various downwind distances from the BTRR site in different atmospheric stability classes (A-F) during the rainy season are also shown in Figure 11 to consider various weather stability effects. From Figure 11, a maximum TEDE of 5.5×10^{-9} Sv is observed for stability class A during the rainy season.

Here, Figure 12 presents the ground deposition activity (kBq/m^2) values in both the plume contour and plume centerline as a function of downwind distance during the rainy season in stability class E for a wind speed of 2.841 m/sec. From Figure 12, it is observed that the maximum ground deposition activity (kBq/m^2) value of 6×10^{-02} kBq/m^2 for stability class E is found at 0.92 km distance for wind from the South direction during the rainy season. Ground deposition values are observed to be 1×10^{-02} kBq/m^2 at 1.2 km^2, 1×10^{-03} kBq/m^2 at 32 km^2, and 1×10^{-04} kBq/m^2 at 240 km^2 from the ground

deposition plume contour curve during the rainy season. According to Figure 12, the values of ground deposition activity increase first, reach a maximum, and subsequently drop with increasing distance during the rainy season.

The results for calculated ground deposition activity at various downwind distances from the BTRR site in different atmospheric stability classes (A-F) during the rainy season are also shown in Figure 13 to consider various weather stability effects. From Figure 13, a maximum ground deposition activity of 1.9×10^{-01} kBq/m^2 is observed for stability class A during the rainy season.

Here, Figure 14 presents the Google earth map illustration for both the TEDE (Sv) contour and the ground deposition (kBq/m^2) contour during the rainy season. We have plotted TEDE (Sv) plume contour and ground deposition (kBq/m^2) contour areas in Google earth pro, as shown in Figure 14, indicating the actual areas impacted by ^{41}Ar dispersion during the rainy season.

The output of the HotSpot 3.1.2 code is shown in Table 8 for distances ranging from 0.03 to 20 km during the rainy

Plume Contour - TED (Sv)

Inner:
1.0E–09 Sv (0.15 km2)
Middle:
1.0E–10 Sv (7.1 km2)
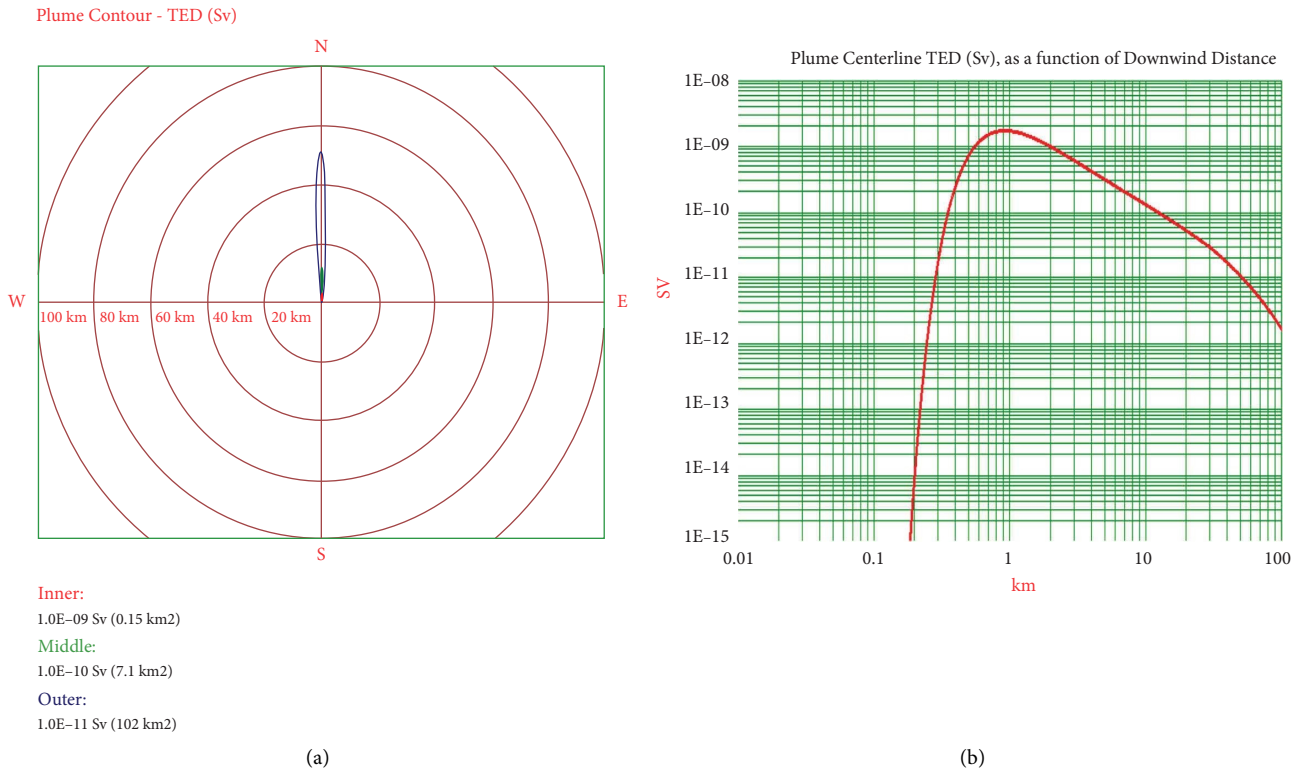Outer:
1.0E–11 Sv (102 km2)

(a)

(b)

FIGURE 10: TEDE (Sv) dose: (a) plume contour and (b) plume centerline as a function of downwind distance during the rainy season in stability class E for the wind speed of 2.841 m/sec.
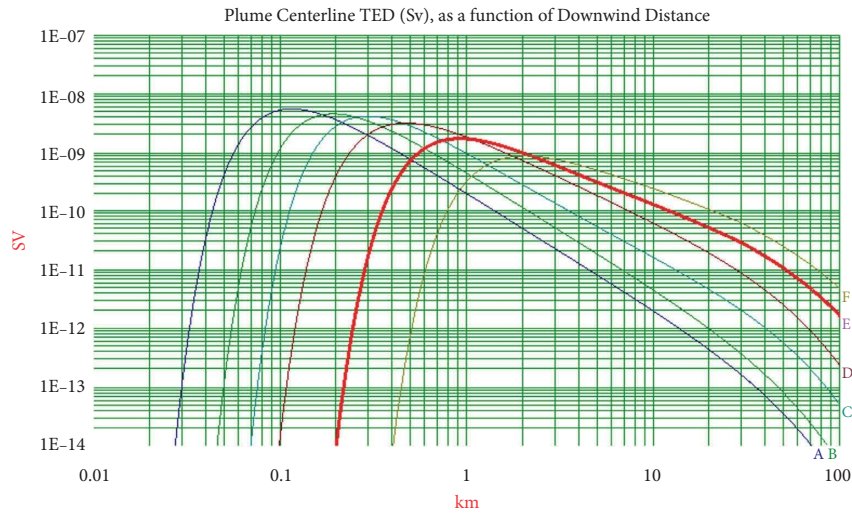

FIGURE 11: TEDE (Sv) dose as a function of downwind distance during the rainy season in different atmospheric stability classes (A–F).

season. From Table 8, the maximum dose was determined at 0.90 km distance during the rainy season. The maximum TEDE, respirable time-integrated air concentration, ground surface deposition, and ground shine dose rate are observed to be 1.8×10^{-9} Sv, 1.8×10^{4} (Bq-sec)/m³, 5.5×10^{-2} kBq/m², and 2.4×10^{-10} Sv, respectively, for ^{41}Ar dispersion during the rainy season. The dose values are found to be very insignificant after 10 km of distance during the rainy season.

Figure 15 represents the organ dose values contributed by the ^{41}Ar radionuclide during the rainy season. Several organs, including the skin, surface bone, breast, lung, red marrow, testes, brain, thyroid, liver, and uterus, have been taken into consideration during the rainy season for dose

Plume Contour - Ground Deposition (kBq/m2)

Inner:
1.00E−02 kBq/m2 (1.2 km2)
Middle:
1.00E−03 kBq/m2 (32 km2)
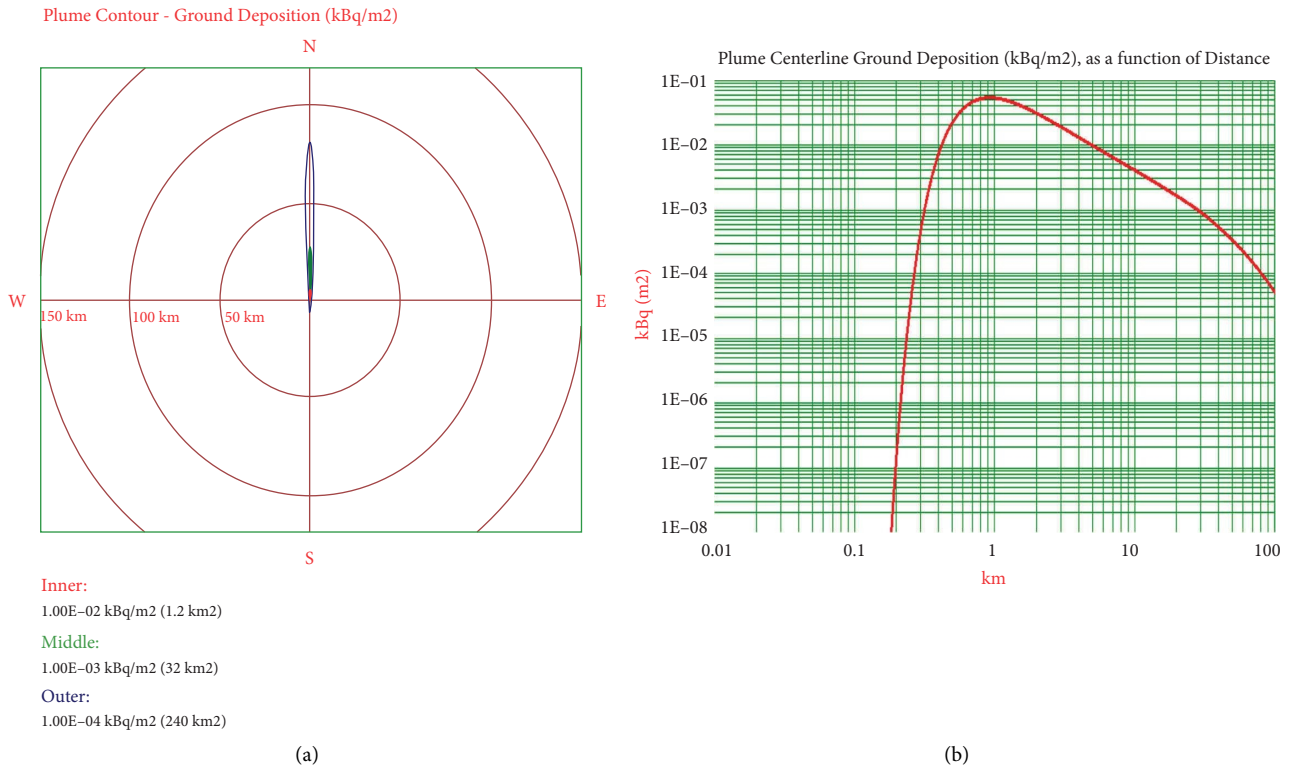Outer:
1.00E−04 kBq/m2 (240 km2)

(a)

(b)

Figure 12: Ground deposition: (a) plume contour and (b) plume centerline activity as a function of downwind distance during the rainy season in stability class E for the wind speed of 2.841 m/sec.
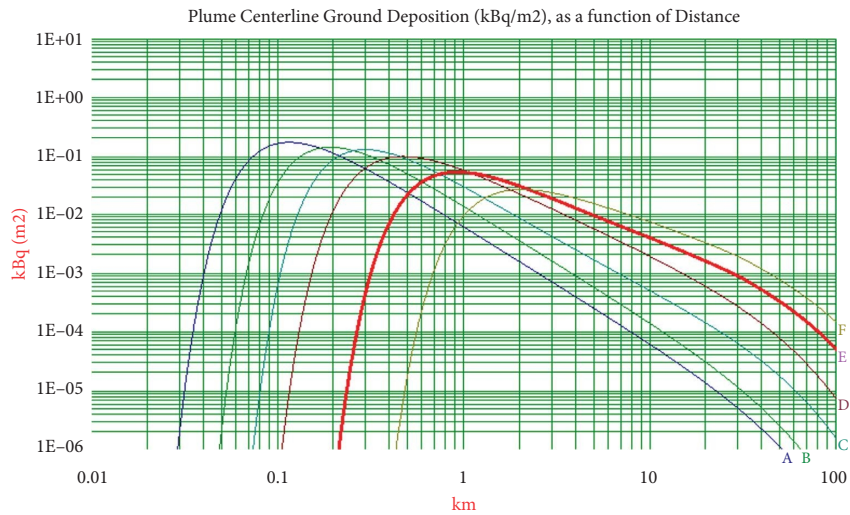
Figure 13: Ground deposition activity as a function of downwind distance during the rainy season in different atmospheric stability classes (A–F).

evaluation based on the results of HotSpot 3.1.2. From Figure 15, it is observed that skin is the highest dose absorber of 4.9×10^{-9} Sv at 0.90 km distance compared to other organs during the rainy season. The obtained dose value for skin during the rainy season is also found to be very negligible compared to the public exposure dose limit for skin of 50 mSv, as shown in Table 7.

Table 9 contains different pathways dose values during both the summer and rainy seasons. From Table 9, the obtained maximum submersion dose (Sv) and ground shine
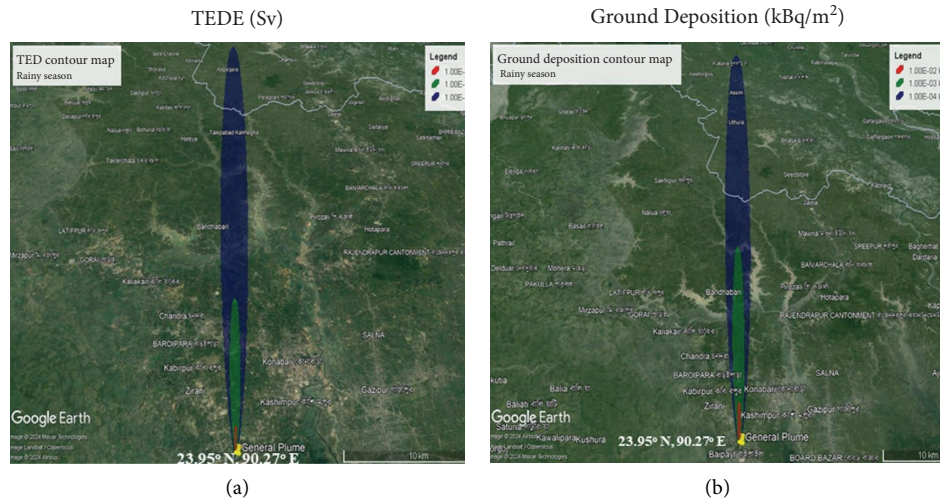
FIGURE 14: Google earth map illustration of (a) TEDE contour and (b) ground deposition (kBq/m^2) contour during the rainy season.

TABLE 8: HotSpot 3.1.2 outputs for the general plume scenarios during the rainy season.

Distance (km)	TEDE (Sv)	Respirable time-integrated air concentration (Bq-sec)/m^3	Ground surface deposition (kBq/m^2)	Ground shine dose rate (Sv/hr)	Arrival time (hour:min)
0.030	$0.0E+00$	$0.0E+00$	$0.0E+00$	$0.0E+00$	<00:01
0.100	$0.0E+00$	$0.0E+00$	$0.0E+00$	$0.0E+00$	<00:01
0.200	$1.4E-14$	$1.8E-01$	$2.3E-07$	$1.0E-15$	<00:01
0.300	$2.3E-11$	$2.6E+02$	$6.2E-04$	$2.7E-12$	00:01
0.400	$2.7E-10$	$2.9E+03$	$8.1E-03$	$3.5E-11$	00:01
0.500	$7.7E-10$	$8.1E+03$	$2.3E-02$	$1.0E-10$	00:01
0.600	$1.2E-09$	$1.3E+04$	$3.8E-02$	$1.7E-10$	00:02
0.700	$1.6E-09$	$1.6E+04$	$4.8E-02$	$2.1E-10$	00:02
0.800	$1.7E-09$	$1.8E+04$	$5.3E-02$	$2.3E-10$	00:03
0.900	$1.8E-09$	$1.8E+04$	$5.5E-02$	$2.4E-10$	00:03
1.000	$1.7E-09$	$1.8E+04$	$5.4E-02$	$2.4E-10$	00:03
2.000	$9.9E-10$	$1.0E+04$	$3.1E-02$	$1.4E-10$	00:07
4.000	$4.2E-10$	$4.4E+03$	$1.3E-02$	$5.7E-11$	00:15
6.000	$2.5E-10$	$2.6E+03$	$7.8E-03$	$3.4E-11$	00:23
8.000	$1.7E-10$	$1.8E+03$	$5.4E-03$	$2.4E-11$	00:31
10.000	$1.3E-10$	$1.4E+03$	$4.1E-03$	$1.8E-11$	00:38
20.000	$5.2E-11$	$5.4E+02$	$1.6E-03$	$7.1E-12$	01:17

dose (Sv) are found to be 2.58×10^{-9} Sv and 1.46×10^{-9} Sv, respectively, at 0.20 km distance during the summer season. It is also determined that during the rainy season, the maximum submersion dose (Sv) and ground shine dose (Sv) are found to be 1.11×10^{-9} Sv and 6.28×10^{-10} Sv, respectively, at 1.0 km distance. There is no inhalation pathway dose contributed by the noble gas ^{41}Ar.

It can be stated that our present study covers the assessment of detailed radiological doses due to the environmental release of ^{41}Ar activity from the BTRR to evaluate the radiological impact on public health and the environment. For dose evaluation, the well-known Health Physics code HotSpot 3.1.2 was used. As a limitation of the current study, a comparative investigation of our HotSpot 3.1.2 results with other established Health Physics codes under the same weather conditions and with same reactor parameters would be more effective.
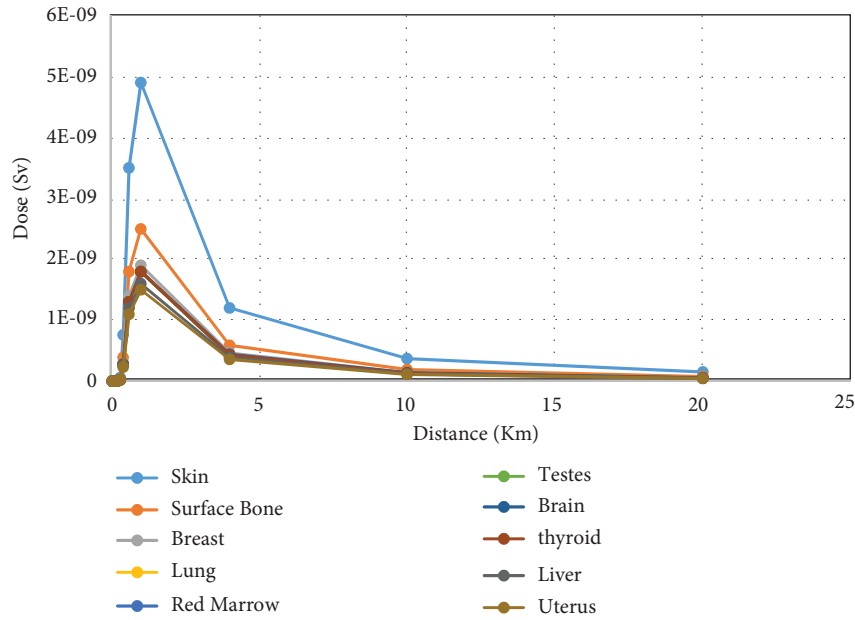
FIGURE 15: Organ-committed dose (Sv) as a function of downwind distance for Pasquill stability class E during the rainy season.

TABLE 9: Different pathways dose data as a function of distance evaluated by HotSpot 3.1.2 code during the summer and rainy seasons.

Distance (km)	Summer		Rainy	
	Submersion-plume passage (Sv)	Ground shine (Sv)	Submersion-plume passage (Sv)	Ground shine (Sv)
0.10	7.08×10^{-10}	3.81×10^{-10}	0.00	0.00
0.20	2.58×10^{-9}	1.46×10^{-9}	1.10×10^{-14}	2.70×10^{-15}
0.30	1.90×10^{-9}	1.07×10^{-9}	1.57×10^{-11}	7.15×10^{-12}
0.40	1.28×10^{-9}	7.22×10^{-10}	1.79×10^{-10}	9.36×10^{-11}
0.60	6.45×10^{-10}	3.65×10^{-10}	7.97×10^{-10}	4.43×10^{-10}
1.0	2.49×10^{-10}	1.41×10^{-10}	1.11×10^{-9}	6.28×10^{-10}
4.0	1.65×10^{-11}	9.30×10^{-12}	2.68×10^{-10}	1.51×10^{-10}
10.0	2.62×10^{-12}	1.48×10^{-12}	8.38×10^{-11}	4.74×10^{-11}
20.0	5.93×10^{-13}	3.35×10^{-13}	3.32×10^{-11}	1.88×10^{-11}

4. Conclusion

The main activity of noble gases produced by the BTRR during normal operation conditions consists of ^{41}Ar, which is continuously released into the atmosphere through the stack. Following its release from the stack, radioactive ^{41}Ar travels offsite with local air flows, potentially exposing people and the environment to gamma radiation released during ^{41}Ar decay. From the point of view of a radiological hazard, gamma rays can cause radiation damage to human organs. Therefore, radiological safety assessment by evaluating radiological doses due to the atmospheric release of ^{41}Ar activity from the BTRR has been carried out using HotSpot 3.1.2 code under different weather conditions. During normal operating conditions of the BTRR, a number of characteristics have an impact on the population's total effective dose equivalent (TEDE). The wind speed at the reactor site affects the TEDE values at different downwind distances. As wind speed increases, the maximum TEDE falls, which also varies with atmospheric stability conditions. Under the present study, long-term meteorological data for the country's two dominant seasons (summer and rainy)

with different atmospheric stability classes (A-F) have been taken into consideration to evaluate weather effects on radiological doses resulting from the ^{41}Ar activity released from the BTRR. During both the seasons, South has been observed as the dominant direction from the wind frequency data. For ensuring radiological safety, a detailed evaluation of TEDE, ground deposition activity, organ-committed dose, and pathways dose have been investigated to determine whether the obtained dose values are within the permissible limit or not. The maximum TEDE is investigated to rise with unstable atmospheric conditions. Comparing to the seasonal findings, a maximum TEDE value of 4.06×10^{-9} Sv has been found during the summer season compared to the rainy season. From the pathways dose results, the maximum submersion and ground shine dose values of 2.58×10^{-9} Sv and 1.46×10^{-9} Sv, respectively, have been found during the summer season compared to the rainy season. According to the computational results for the atmospheric release of ^{41}Ar activity, the highest TEDE values surrounding the BTRR site have been obtained less than the annual effective dose limits for workers and the population, suggested by the international standards. Thus, we can draw

the conclusion that the BTRR site has reasonably attained the standards of safety based on established protocols as outlined in the regulatory guidance. As a recommendation for future research, more studies on radiological dose analysis using advanced computational codes might be carried out to examine the radiological safety of research-type nuclear reactors in accordance with regulatory authority guidelines.

Data Availability

The data employed in this study to underpin our findings can be obtained from the corresponding author upon request by e-mail, arifstyn@yahoo.com.

Conflicts of Interest

The authors declare that there are no conflicts of interest regarding the publication of this article.

References

[1] M. A. Hoq, M. M. Soner, A. Rahman, M. A. Salam, and S. M. A. Islam, "Estimation of ^{41}Ar activity concentration and release rate from the TRIGA Mark-II research reactor," *Journal of Environmental Radioactivity*, vol. 153, pp. 68–72, 2016.

[2] M. A. Hoq, M. A. M. Soner, M. A. Salam, M. M. Rahman, and N. Jahan, "Experimental study of ^{41}Ar activity release rate from the Bangladesh atomic Energy commission TRIGA research reactor," *International Journal of Nuclear Energy Science and Technology*, vol. 14, no. 1, pp. 71–81, 2020.

[3] M. A. Malek, K. J. A. Chisty, and M. M. Rahman, "Dose distribution of ^{131}I, ^{132}I, ^{133}I, ^{134}I, and ^{135}I due to a hypothetical accident of TRIGA Mark-II research reactor," *International Journal of Basic and Applied Sciences*, vol. 1, no. 3, pp. 244–259, 2012.

[4] M. A. Khaer, M. Hoq, S. M. T. Hassan, M. T. Chowdhury, and M. M. Rahman, "Assessment of radiological dose and emergency planning zones of TRIGA Mark-II research reactor of Bangladesh due to a postulated severe accidental condition," *Nuclear Engineering and Design*, vol. 415, Article ID 112727, 2023.

[5] M. R. Mawla, A. Rahman, A. Sattar, R. Ryean, and I. M. Shafiqul, "Assessment of radiological consequences to a hypothetical accident of the 3-MW TRIGA research reactor of Bangladesh," 2024.

[6] A. F. M. M. Rahman, M. Shamsuzzaman, M. S. Rahman et al., "Assessment of radiological dose around a 3-MW TRIGA mark-II research reactor," *International Letters of Chemistry, Physics and Astronomy*, vol. 15, pp. 183–200, 2013.

[7] D. Mladin, M. Mladin, A. Toma, C. Dulama, I. Prisecaru, and S. Covaci, "Calculation of radioactive species transport in a TRIGA reactor," *Nuclear Engineering and Design*, vol. 262, pp. 29–38, 2013.

[8] M. Fukui, "Twenty years of experience in monitoring ^{41}Ar in a research reactor and decrease of its discharge into the environment," *Health Physics*, vol. 86, no. 4, pp. 384–396, 2004.

[9] dataportal, "Bangladesh meteorological department (bmd), dhaka," 2023, https://dataportal.bmd.gov.bd.

[10] Narac, *National Atmospheric Release Advisory Center Lawrence Livermore National Laboratory Livermore*, University of California, Los Angeles, CA, USA, 2020.

[11] M. A. Zulquarnain, M. M. Haque, M. A. Salam et al., "Experience with the operation, maintenance and utilisation of the 3 MW TRIGA Mark-II research reactor of Bangladesh," *International Journal of Nuclear Energy Science and Technology*, vol. 4, no. 4, pp. 299–312, 2009.

[12] A. M. Soner, A. A. Mahmud, M. Hossain et al., "BAEC TRIGA research reactor: 35 years' experience," *International Journal of Nuclear Energy Science and Technology*, vol. 16, no. 1, pp. 1–20, 2022.

[13] Atomic Energy Research Establishment, *Technical Report, AERE/TR-27*, Atomic Energy Research Establishment (AERE), Mumbai, India, 2021.

[14] International Atomic Energy Agency, *Generic Models and Parameters for Assessing the Environmental Transfer of Radionuclides from Routine Releases, Procedures and Data*, IAEA-SS-57, Vienna, Austria, 1982.

[15] IAEA, *Derivation of the Source Term and Analysis of the Radiological Consequences of Research Reactor Accidents (SRS No. 53)*, IAEA-SS-57, Vienna, Austria, 2008.

[16] International Commission on Radiological Protection, "Human respiratory tract model for radiological protection, icrp 66," *Annals of ICRP*, vol. 24, pp. 1–3, 1994.

[17] International Commission on Radiological Protection, "Age dependent doses to the members of the public from intake of radionuclides, icrp 72," *Annals of ICRP*, vol. 26, p. 1, 1996.

[18] IAEA, *General Safety Requirements, GSR Part 3*, IAEA, Vienna, Austria, 2014.

[19] ICRP, "Recommendations of the international commission on radiological protection," *ICRP Publication 60. Ann. ICRP*, vol. 21, no. 1-3, 1991.

[20] ECFR, "10 cfr Part 20," 2023, https://www.ecfr.gov/current/title-10/chapter-I/part-20.